Available online at www.sciencedirect.com
SCIENCE DIRECT®
Talanta 65 (2005) 1091–1096
Talanta
www.elsevier.com/locate/talanta

Molecular orientation of azobenzene chromophores in ultrathin polymer nanosheets studied by attenuated total reflection spectroscopy

Masaya Mitsuishi*, Tomohiro Tanuma, Jun Matsui, Tokuji Miyashita

Institute of Multidisciplinary Research for Advanced Materials (IMRAM), Tohoku University, Katahira 2-1-1, Aoba-ku, Sendai 980-8577, Japan

Received 26 January 2004; received in revised form 17 April 2004; accepted 28 April 2004
Available online 23 November 2004

Abstract

This paper describes characterization of molecular orientation for azobenzene moieties in a polymer nanosheet. Copolymers of *N*-[4-(phenylazo)phenyl] acrylamide (PAZoA) with *tert*-pentyl acrylamide (tPA) were synthesized and the monolayers deposited on tapered quartz waveguides by Langmuir–Blodgett (LB) technique. Spectroscopic properties of the copolymer (p(tPA/PAZoA)) monolayers were monitored by integrated optical waveguide technique on the molecular level. Molecular orientation of the azobenzene was precisely determined by polarized absorption spectra. It was found that the azobenzene groups took a horizontal orientation and distributed uniformly in the p(tPA/PAZoA) monolayer without significant PAZoA aggregation. Photoisomerization process from *trans* to *cis* form was also investigated. More than half of the *trans* form (60–70%) was photoisomerized under unpolarized light irradiation, and the photoisomerization rate was independent on the PAZoA contents. This implies that the microenvironment of PAZoA moieties was almost the same in three different p(tPA/PAZoA) monolayers.

Keywords: Polymer; Waveguide; Nanosheet; LB film; Azobenzene

1. Introduction

Azobenzene is a promising material for photonic devices such as optical information storage, light switching devices, and nonlinear optical devices [1–4]. The deep understanding of the photoisomerization mechanism [5], especially from a perspective of changes in molecular orientation, brings further possibility for future application. Many researchers have intensively investigated molecular orientation of azobenzene derivatives confined in thin films and their photochromic properties have been examined using spectroscopic tools such as UV–vis spectroscopy, FT-IR spectroscopy, and surface plasmon spectroscopy [6,7].

Recently, much effort has been devoted to construct functional nanoassemblies including supramolecules. Azobenzene derivatives have been successfully incorporated into nanoassemblies, e.g. self-assembled monolayers [8–10], layer-by-layer assemblies [11–13], and Langmuir–Blodgett (LB) films [14–16]. Many approach based on these techniques have proved fascinating azobenzene nano-assembly fabrication, and it is also inevitable to design molecular systems so that azobenzene molecules can undergo large changes in structure even at the nanometer scale [10].

The LB technique provides deposition of ultrathin layer assemblies at the molecular scale. Besides, the chromophores align themselves into an ordered structure. We found that poly(alkyl acrylamide) LB monolayer took a highly ordered and stable monolayer formation at the water surface with its monolayer thickness in the range of 1–2 nm [17,18]. The monolayer is transferred onto solid supports and various functional groups can be confined in the nanostructure with high orientation and desired arrangement [19]. Molecular orientation has been also studied by choosing suitable alkyl side chains capable of forming stable monolayer at the air–water interface [20].

---

* Corresponding author. Tel.: +81 22 217 5639; fax: +81 22 217 5639.
E-mail address: masaya@tagen.tohoku.ac.jp (M. Mitsuishi).

0039-9140/$ – see front matter © 2004 Elsevier B.V. All rights reserved.
doi:10.1016/j.talanta.2004.04.043

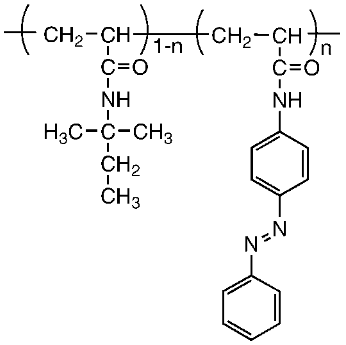

Fig. 1. Chemical structure of p(tPA/PAZoA).

It is important to understand spectroscopic properties of nanoassemblies such as LB films because the information gives insights into organic nanophotonic device fabrication. However, spectroscopic study of ultrathin films by single-pass transmission UV–vis absorption spectroscopy meets difficulty in resolution due to shortage of optical path length. Since Swalen and his colleagues reported monolayer spectroscopic properties in 1978, much attention has been paid to spectroscopy based on waveguide optics [21], optical waveguide (OWG) technique [22–24] has been developed and utilized to study molecular orientation [25,26], electrochemical analysis [27,28] and protein adsorption [29,30], etc. Previously, we demonstrated characterization of photocrosslinking reaction occurred in anthracene-labeled polymer LB films with UV light irradiation [31]. In this paper, amphiphilic copolymers containing azobenzene groups (p(tPA/PAZoA)s) were synthesized and their spectroscopic properties at the monolayer level were investigated. The monolayer was transferred onto a quartz waveguide and molecular orientation of azobenzene in p(tPA/PAZoA) monolayer was characterized with polarized absorption spectra under attenuated total reflection mode. Furthermore, *trans*–*cis* photoisomerization of p(tPA/PAZoA)s was investigated using time-resolved absorption spectra.

2. Experimental

2.1. Materials

N-[4-(Phenylazo)phenyl] acrylamide (PAZoA) was synthesized by a similar procedure described elsewhere [32]. Copolymers of *tert*-pentyl acrylamide (tPA) with different PAZoA contents were synthesized by free radical polymerization in toluene for 24 h (Fig. 1). Mole content of PAZoA group was determined with UV–vis absorption spectroscopy, using molar extinction coefficient of PAZoA ($2.75 \times 10^4\ \mathrm{M^{-1}\,cm^{-1}}$ at 350 nm) in chloroform as reference. The molecular weights (number-averaged and weight-averaged molecular weights (M_n and M_w)) were determined by gel permeation chromatography using a polystyrene standard. They are summarized in Table 1. Spectroscopic grade chloroform was used as spreading solvent. Pure distilled water with a resistivity higher than 17.5 MΩ cm (purified by a CPW-10 system (Advantec)) was used as the subphase.

Table 1
Characterization of p(tPA/PAZoA) copolymers

Copolymer	PAZoA contents (mol%)	$M_n \times 10^{-4}$	M_w/M_n	PAZoA area (nm^2)
p(Tpa/PAZoA5)	5.0	1.95	1.30	0.98
p(tPA/PAZoA10)	10.4	1.37	1.44	0.78
p(tPA/PAZoA19)	18.5	0.81	1.65	0.61

2.2. Attenuated total reflection spectroscopy

A quartz slide (thickness ca. 200 μm, 65 mm × 20 mm, USI) tapered at both sides by 60° was used as a substrate. The substrate was rinsed with methanol for 30 min, treated with ultrasonication for 10 min. After rinsed with distilled water, the substrate was made hydrophilic with a UV-O_3 cleaner (NL-253, Nippon Laser Electronics). Surface pressure (π)–area (A) isotherm measurements and LB film deposition of p(tPA/PAZoA) monolayers were performed using a Langmuir trough (HBM, Kyowa Interface Science, Co. Ltd.). The monolayer was transferred on the waveguide surface by the vertical dipping method keeping surface pressure and temperature at 20 mN/m and 20 °C, respectively. Absorption spectra of p(tPA/PAZoA) LB films were measured by a surface and interface spectrometer (SIS-50, System Instruments Co. Ltd.). The experimental setup is schematically illustrated in Fig. 2. White light from a 150 W Xe lamp was utilized as a signal. The light impinges in the tapered quartz substrate through a quartz fiber. Optical waves propagate in the quartz slide, undergoing total internal reflection at the slide interface. The output signal was collected by a CCD spectrograph and spectra were stored in a personal computer. This allows recording of absorption spectra in the range of wavelengths from 250 to 800 nm. For photochemical reaction observation, a deep UV lamp (MDX-500MA, USHIO) was utilized as an irradiation source. The waveguide surface was

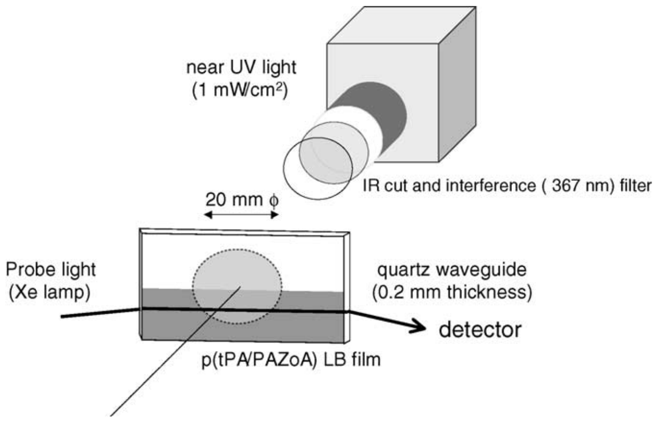

Fig. 2. Experimental setup for attenuated total reflection spectroscopy.

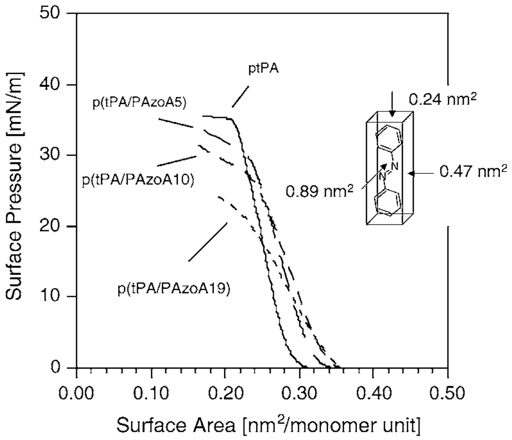

Fig. 3. Surface pressure (π)–area (A) isotherms of p(tPA/PAZoA) monolayers measured at 20 °C.

irradiated with monochromatic light (1.0 mW/cm^2) through an IR-cut filter and an interference filter (367 nm). Propagation direction of the near UV light was selected perpendicular to the waveguide plane as shown in Fig. 2. Since the light power was fairly low, effects of the irradiated light on absorption spectra were negligible. Absorption spectra were simultaneously recorded as a function of irradiation time. Measurements were performed under dark condition at room temperature.

3. Results and discussion

3.1. Monolayer formation of p(tPA/PAZoA)s

Fig. 3 shows surface pressure (π)–area (A) isotherms for the p(tPA/PAZoA) LB monolayers, which contains 5, 10, and 19 mol% of PAZoA, respectively. For comparison, the isotherm of homopolymer, ptPA is shown in Fig. 3. The collapse pressure decreased as PAZoA contents increased. Averaged limiting surface area, estimated by extrapolating the linear portion of the condensed state in the π–A isotherms to zero surface pressure, was increased with increasing PAZoA contents. As PAZoA contents increase, it is likely that the monolayers take an unstable monolayer formation. The limiting surface areas for PAZoA groups were determined (Table 1), assuming that those for tPA are 0.28 nm^2 [12]. A comparison of these results with the calculated values based on the CPK model (inset, Fig. 3) suggests that the azobenzene groups take a fairly parallel orientation to the water surface plane at the air–water interface. These monolayers can be transferred onto solid supports by vertical dipping method. The transfer ratio of p(tPA/PAZoA) monolayers are listed in Table 2. Although the transfer ratio of p(tPA/PAZoA19) at the down-stroke was relatively lower (DOWN, 0.5), the p(tPA/PAZoA) monolayer can be transferred in both up- and down-strokes as Y-type LB films. For further investigation, the p(tPA/PAZoA) monolayers were transferred in the up-stroke onto waveguide surface so that the hydrophobic portion was exposed to the surface.

Table 2
Transfer ratio of p(tPA/PAZoA) monolayers onto solid substrates

Copolymer	Down	Up
p(tPA/PAZoA5)	0.8	1.0
p(tPA/PAZoA10)	0.8	1.0
p(tPA/PAZoA19)	0.5	0.8

Fig. 4 shows absorption spectra for p(tPA/PAZoA) monolayers with unpolarized probed light. The characteristic band (π–π transition moment of *trans*-azobenzene) of PAZoA groups is clearly observed around near 350 nm [33,34]. Besides, the absorbance increased with PAZoA contents. This proves that the p(tPA/PAZoA) monolayers were transferred on the waveguide with the transfer ratio of almost unity. In comparison with absorption spectra of the p(tPA/PAZoA5) LB monolayer measured by a transmission UV–vis spectrophotometer (dashed line, Fig. 4), the optical waveguide measurement clearly provides us with greatly enhanced sensitivity. Sensitivity increased approximately by a factor of 100. This allows us to analyze molecular orientation of p(tPA/PAZoA) monolayers at the molecular level.

3.2. Molecular orientation of azobenzene chromophores in p(tPA/PAZoA) monolayer

The absorption of a dye monolayer depends strongly on the orientation of the transition moments with respect to the direction of the electric vector of the incident light wave. As shown in Fig. 4, the azobenzene has its characteristic bands around 350 nm. This corresponds to the *trans*-azobenzene's absorption band in which the transition moment orients parallel to the molecular long axis [33,34]. Considering the experimental axes in relation to the cross section of the waveguide substrate and the plane of incidence (Fig. 5), the electric field

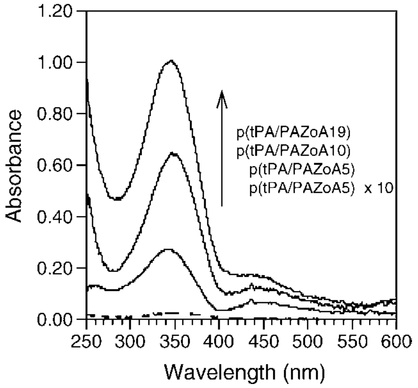

Fig. 4. Absorption spectra for p(tPA/PAZoA) monolayers monitored by attenuated total reflection spectroscopy. The dashed line corresponds to spectrum of p(tPA/PAZoA5) monolayer monitored by transmission UV–vis spectroscopy.

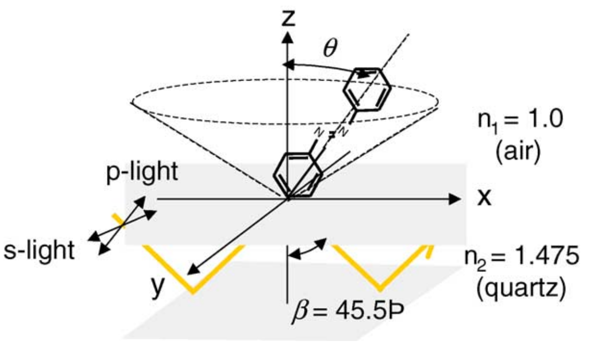

Fig. 5. Schematic illustration of molecular orientation definition on the waveguide surface.

amplitudes at the surface are given in Eq. (1) [35]

$$E_x = \frac{2(\sin^2\beta - n_{21}^2)^{1/2}\cos\beta}{(1-n_{21}^2)^{1/2}[(1+n_{21}^2)\sin^2\beta - n_{21}^2]^{1/2}},$$

$$E_y = \frac{2\cos\beta}{(1-n_{21}^2)^{1/2}},$$

$$E_z = \frac{2\sin\beta\cos\beta}{(1-n_{21}^2)^{1/2}[(1+n_{21}^2)\sin^2\beta - n_{21}^2]^{1/2}} \tag{1}$$

where E_i ($i = x, y$, and z) is electric field amplitudes in the three Cartesian directions at the surface, β the propagation angle in the waveguide, $n_{21}(n_2/n_1)$ the ratio of refractive index of two dielectric media. The dichroic ratio of TE (s-light) absorption to TM (p-light) can be related to the orientation angle of dye molecule by [35]

$$\frac{A_\mathrm{s}}{A_\mathrm{p}} = \frac{|E_y|^2}{|E_x|^2 + 2|E_z|^2\cot^2\theta} \tag{2}$$

where A_s and A_p are polarized absorbance, and θ the orientation angle between the transition moment vector and the z-axis. This assumes that dye molecules take a rotationally symmetric distribution in the waveguide plane (Fig. 5). Polarized absorption spectra for p(tPA/PAZoA10) monolayer are shown in Fig. 6(a). Fig. 6(a) shows significant anisotropic absorption of p(tPA/PAZoA10) monolayer; the absorbance for s-light at 350 nm is larger than that for p-light. Qualitatively, this suggests that the azobenzene takes a parallel orientation to the waveguide plane. For two other p(tPA/PAZoA) monolayers, similar results were obtained. In a similar approach reported by Menzel et al. [36], we tried to decompose absorption band around 350 nm to estimate the amount of azobenzene aggregates: monomer, H-aggregates, and J-aggregates [37]. We assumed that these components have its maximum

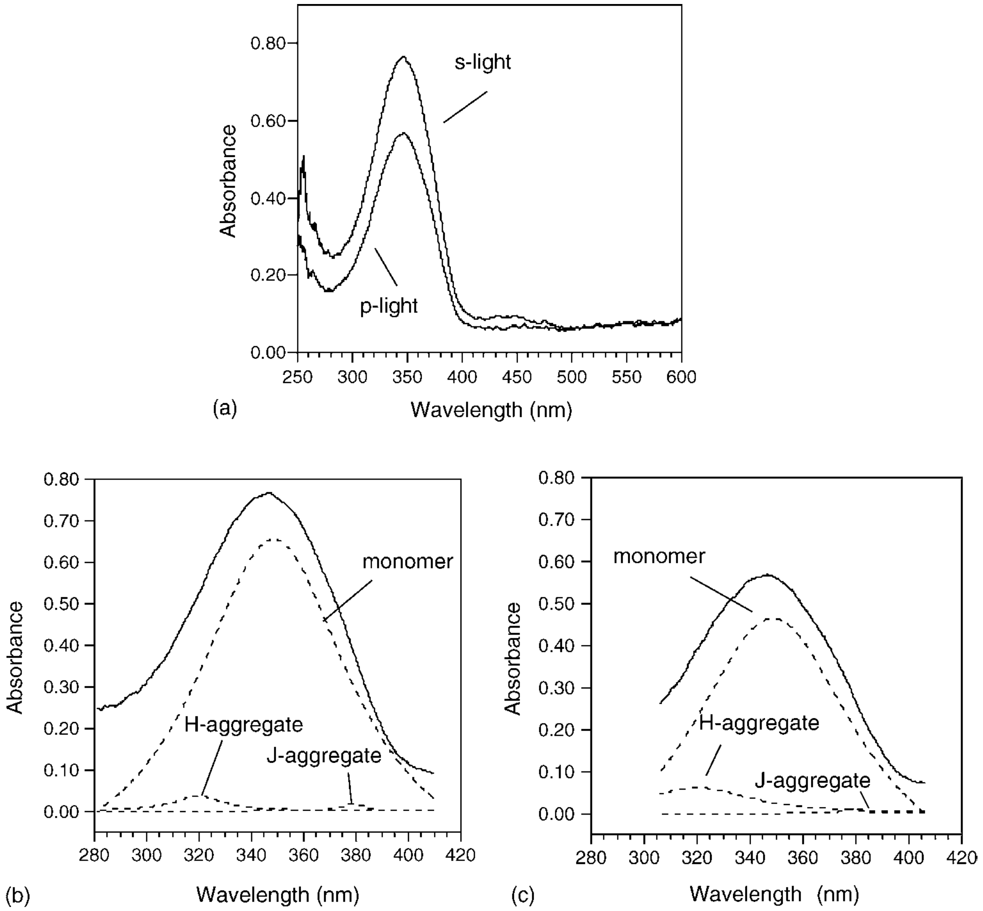

Fig. 6. Polarized absorption spectra for p(tPA/PAZoA10) monolayer (a), spectrum decomposition for s-light (b) and p-light (c).

Table 3
Percentage of different aggregates in p(tPA/PAZoA) monolayers calculated by absorption spectra decomposition

Copolymer	Integrated area for p-light (%)			Integrated area for s-light (%)		
	H-aggregate	Monomer	J-aggregate	H-aggregate	Monomer	J-aggregate
p(tPA/PAZoA5)	5.2	91.6	3.1	2.7	97.3	0.0
p(tPA/PAZoA10)	5.3	94.4	0.3	1.7	97.8	0.4
p(tPA/PAZoA19)	7.8	91.8	0.4	3.3	96.0	0.6

Table 4
Dichroic ratio and orientation angle of different aggregates in p(tPA/PAZoA) monolayers

	H-aggregate		Monomer		J-aggregate	
	A_s/A_p	θ (°)	A_s/A_p	θ (°)	A_s/A_p	θ (°)
p(tPA/PAZoA5)	0.71	57.1	1.38	71.9	–[a]	–[a]
p(tPA/PAZoA10)	0.58	53.1	1.24	69.2	1.9	82.8
p(tPA/PAZoA19)	0.71	57.1	1.35	71.3	1.9	82.8

[a] Not obtainable.

at 348.5, 320, and 379 nm, respectively, and the spectrum was fitted with Lorentzian type absorption bands (see for example [38]), keeping all parameters constant except the amplitudes of the peaks. As shown in Fig. 6(b) and (c), the spectra were reproducibly assigned (within 3% experimental error). Interestingly, there are no significant absorption bands of H-aggregates and J-aggregates for both polarized absorption spectra. The integrated area of each absorption band, dichroic ratio and molecular orientation angle obtained from Eqs. (1) and (2) are summarized in Tables 3 and 4. Comparing the results with those reported by Menzel et al. (‘hairy-rod’ polymer LB films) [36], these are significant differences. In the hairy-rod LB films, the amount of H-aggregates ranged from 27 to 46% and the values were comparable to those of monomer. The use of azobenzene homopolymer and multilayer structure seems to bring close proximity arrangement of azobenzene side chains. In the p(tPA/PAZoA) monolayer, however, the azobenzene contents is at most ca. 20% in the two dimensional nanosheet. The PAZoA moieties are separated from each other, resulting in no significant aggregates formation. As for the orientation angle shown in Table 4, it must be mentioned that the orientation angle can be determined with uncertainty of 1.5°. The orientation angle for PAZoA monomer was determined to be around 70.0°. Although the peak fitting is not a real quantitative determination, it is interesting that the orientation angle for H- and J-aggregates reflects their orientation. From these findings, we can conclude that the azobenzene group takes a parallel orientation and uniformly distributed without significant aggregate formation in the p(tPA/PAZoA) monolayer.

3.3. Photoisomerization reaction in p(tPA/PAZoA) monolayer

The attracting features of azobenzene are based on photoisomerization reaction from thermodynamically stable *trans* to *cis* configuration by irradiation of near UV light. These processes are reversible; azobenzene changes its form from *trans* to *cis* with UV light irradiation, from *cis* to *trans* with visible light irradiation or heating. We investigated photoisomerization process from *trans* to *cis* form in the p(tPA/PAZoA)

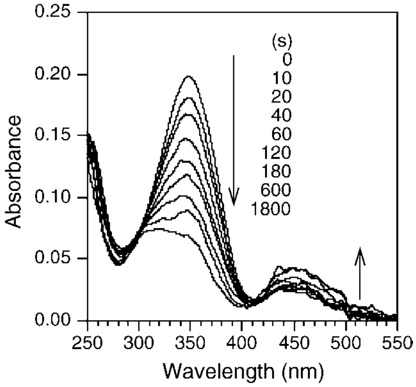

Fig. 7. Absorption spectra change for p(tPA/PAZoA10) monolayer as a function of irradiation time.

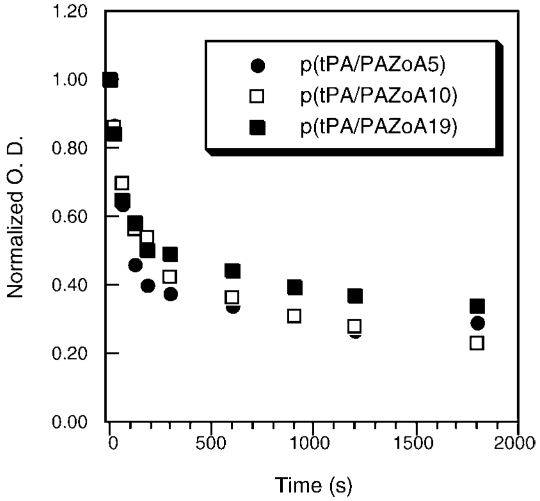

Fig. 8. Plots of normalized absorbance change at 350 nm.

monolayer. Fig. 7 shows changes in absorption spectra of the p(tPA/PAZoA10) monolayer as a function of irradiation time. During the measurement the surroundings were kept dark to prevent the reverse photochemical reaction. The spectra in Fig. 7 were obtained by correcting each absorption spectrum to show the absorbance change at irradiated part only (Fig. 2). As the irradiation proceeds, the absorption band at 350 nm drastically decreased, while new absorption band clearly appeared at 450 nm. The absorbance reached a saturated value within 30 min irradiation. The saturated value was fairly larger than that in chloroform solution (the data is not shown) due to constraint of azobenzene in the solid state.

Plots of absorbance changes are shown in Fig. 8. For clarity, absorbances are normalized at initial values. Interestingly, changes in absorbance were almost the same. In other words, the higher PAZoA contents did not change the photoisomerization rate and conversion yield. This is quite consistent with the result of aggregates analysis mentioned above. This means that the microenviroment of azobenzene is quite similar in p(tPA/PAZoA) monolayers. Provided that no significant absorption band for *cis*-azobenzene appeared at 350 nm, 30–40% of *trans*-azobenzene undergoes no *trans* to *cis* photoisomerization.

In conclusion, we demonstrated high sensitivity of optical waveguide technique for characterization of molecular orientation and photochemical reaction in p(tPA/PAZoA) LB monolayers. Absorption spectra of p(tPA/PAZoA) monolayer was observed with high sensitivity and accuracy, leading to the determination of molecular orientation in the p(tPA/PAZoA) monolayers. It was found that the azobenzene group directs its molecular long axis parallel to waveguide plane (∼70° from surface normal) and uniformly distributed in the p(tPA/PAZoA) monolayers. As for photoisomerization mechanism, the photoisomerization rate and conversion yield shows no dependence on the PAZoA contents. The PAZoA group is located in the hydrophobic side and surrounded by tPA moieties. In other words, the tPA does not constrain the PAZoA motion induced by near UV light. This would be one possible reason for the same changes in absorbance in p(tPA/PAZoA) monolayers. In this paper, we utilized unpolarized light as an irradiation source. The photoisomerization mechanism under polarized light irradiation should be clarified because of its potential for photofunctional application based on dichroic and birefringent properties. The work is now in progress and will be reported in near future.

Acknowledgements

This work was partially supported by a Grant-in-Aid on Priority Areas (Fundamental Science and Technology of Photofunctional Interfaces, No. 417) and Scientific Research (No. 14205130) from the Ministry of Education, Culture, Sports, Science, and Technology of Japan.

References

[1] A. Natansohn, P. Rochon, Chem. Rev. 102 (2002) 4139.
[2] K. Ichimura, Chem. Rev. 100 (2000) 1847.
[3] J.A. Delarire, K. Nakatani, Chem. Rev. 100 (2000) 1817.
[4] M. Dumont, A.E. Osman, Chem. Phys. 245 (1999) 437.
[5] T. Todorov, L. Nikolova, N. Tomova, Appl. Opt. 23 (1984) 4309.
[6] K. Tawa, K. Kamada, K. Kiyohara, K. Ohta, D. Yasumatsu, Z. Sekkat, S. Kawata, Macromolecules 34 (2001) 8232.
[7] E.F. Aust, S. Ito, M. Sawodny, W. Knoll, Trend. Polym. Sci. 2 (1994) 313.
[8] Z. Sekkat, J. Wood, Y. Geerts, W. Knoll, Langmuir 11 (1995) 2856.
[9] K. Ichimura, S.-K. Oh, M. Nakagawa, Science 288 (2000).
[10] K. Tamada, H. Akiyama, T. Wei, Langmuir 18 (2002) 5239.
[11] S. Dante, R. Advincula, C.W. Frank, P. Stroeve, Langmuir 15 (1999) 193.
[12] S. Bian, J.-A. He, L. Li, J. Kumar, S.K. Tripathy, Adv. Mater. 12 (2000) 1202.
[13] I. Suzuki, T. Ishizaki, T. Hoshi, J. Anzai, Macromolecules 35 (2002) 577.
[14] T. Kawai, J. Umemura, T. Takenaka, Langmuir 5 (1989) 1378.
[15] T. Seki, Supramol. Sci. 3 (1996) 25.
[16] J-W. Weener, E.W. Meijer, Adv. Mater. 12 (2000) 741.
[17] T. Miyashita, Y. Mizuta, M. Matsuida, Br. Polym. J. 22 (1990) 327.
[18] T. Taniguchi, Y. Yokoyama, T. Miyashita, Macromolecules 30 (1997) 3646.
[19] T. Miyashita, Prog. Polym. Sci. 18 (1993) 294.
[20] J. Matsui, M. Mitsuishi, T. Miyashita, Macromolecules 32 (1999) 381.
[21] J.D. Swalen, M. Tacke, R. Santo, K.E. Rieckhoff, J. Fischer, Helv. Chim. Acta 61 (1978) 960.
[22] P.W. Bohn, Anal. Chem. 57 (1985) 1203.
[23] K. Kato, A. Takatsu, N. Matsuda, R. Azumi, M. Matsumoto, Chem. Lett. (1995) 437.
[24] T.E. Plowman, S.S. Saavedra, W.M. Reichert, Biomaterials 19 (1998) 341.
[25] K.D. Hughes, M.J. LaBuda, P.W. Bohn, Appl. Opt. 30 (1991) 4406.
[26] P.L. Edmiston, J.E. Lee, L.L. Wood, S.S. Saavedra, J. Phys. Chem. 100 (1996) 775.
[27] K. Ito, A. Fujishima, J. Phys. Chem. 92 (1988) 7043.
[28] K. Fujita, C. Suzuki, H. Ohno, Electrochem. Commun. 5 (2003) 47.
[29] D.S. Walker, M.D. Garrison, W.M. Reichert, J. Colloid Interf. Sci. 157 (1993) 41.
[30] Z.-M. Qi, N. Matsuda, T. Yoshida, H. Asano, A. Takatsu, K. Kato, Opt. Lett. 27 (2002) 2001.
[31] M. Mitsuishi, T. Tanuma, J. Matsui, T. Miyashita, Langmuir 17 (2001) 7449.
[32] K. Arisumi, F. Feng, T. Miyashita, H. Ninomiya, Langmuir 14 (1998) 5555.
[33] D.L. Beveridge, H.H. Jaffé, J. Am. Chem. Soc. 88 (1966) 1948.
[34] P. Uznanski, M. Kryszewski, E.W. Thulstrup, Spectrochim. Acta 46A (1990) 23.
[35] D.M. Cropek, P.W. Bohn, J. Phys. Chem. 94 (1990) 6452.
[36] H. Menzel, B. Weichart, A. Schmidt, S. Paul, W. Knoll, J. Stumpe, T. Fischer, Langmuir 10 (1994) 1926.
[37] M. Kasha, Molecular excitons in small aggregates, In: B. Di Bartolo, (Ed.), Spectroscopy of the Excited State, New York, 1975, pp. 337–361.
[38] K.D. Möller, Optics, University Science Books, California, 1988, p. 284.